Supplementary Information for

Well-defined carbon polyhedrons prepared from nano metal-organic frameworks for oxygen reduction

*Wei Xia, Jinghan Zhu, Wenhan Guo, Li An, Dingguo Xia and Ruqiang Zou**

Beijing Key Lab of Advanced Battery Materials, College of Engineering

Peking University, Beijing 100871, P. R. China

*Corresponding author. Email: rzou@pku.edu.cn

RHE conversion

Cyclic voltammograms (CV) was performed at a scan rate of 1 mV s^{-1} in hydrogen saturated 0.1 M HClO4 with polished Pt wires as the working electrode and counter electrode, and Ag/AgCl (saturated KCl) as the reference electrode. The potential at the point of zero current was taken as the thermodynamic potential for hydrogen electrode reaction.[1]

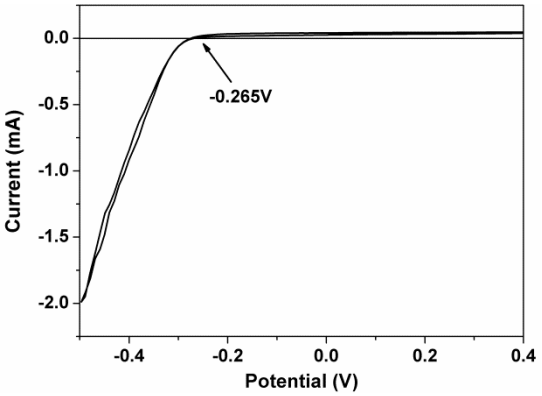

So $V_{RHE} = V_{Ag/AgCl} + 0.265$ V

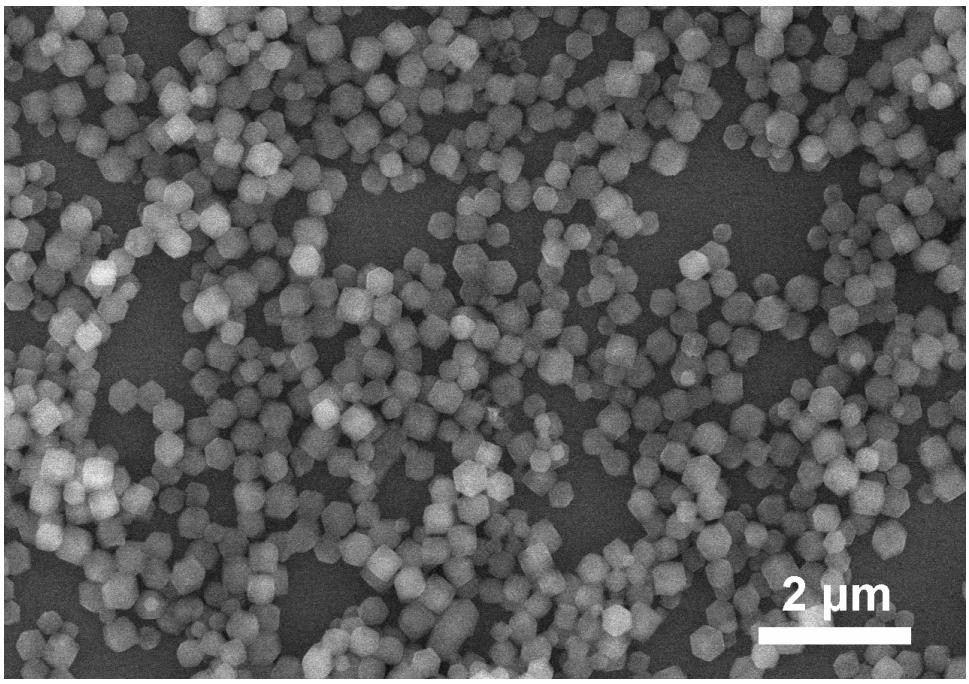

Fig. S1. SEM images of 300 nm ZIF-67.

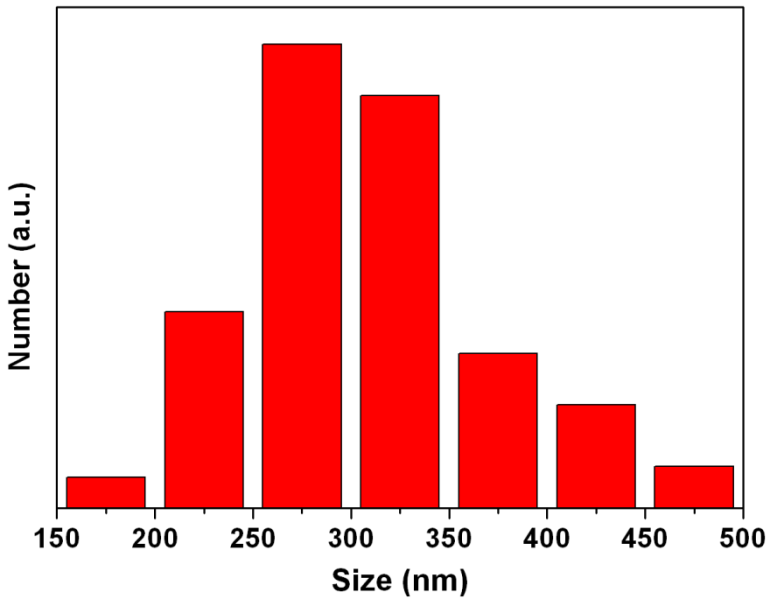

Fig. S2. Size distribution of 300 nm ZIF-67 (from a total number of 400).

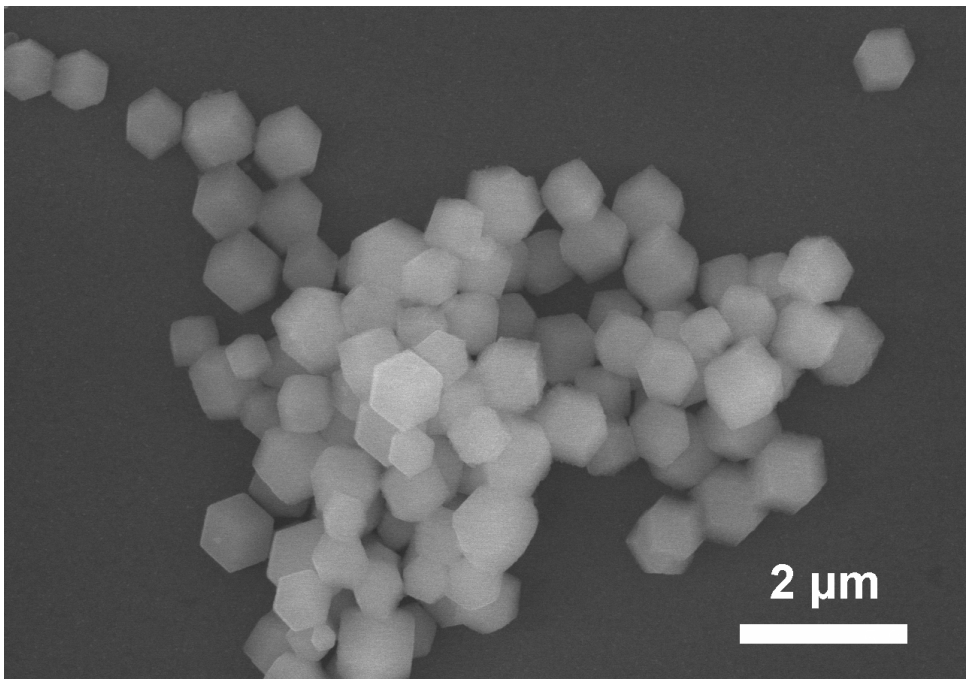

Fig. S3. SEM images of 800 nm ZIF-67.

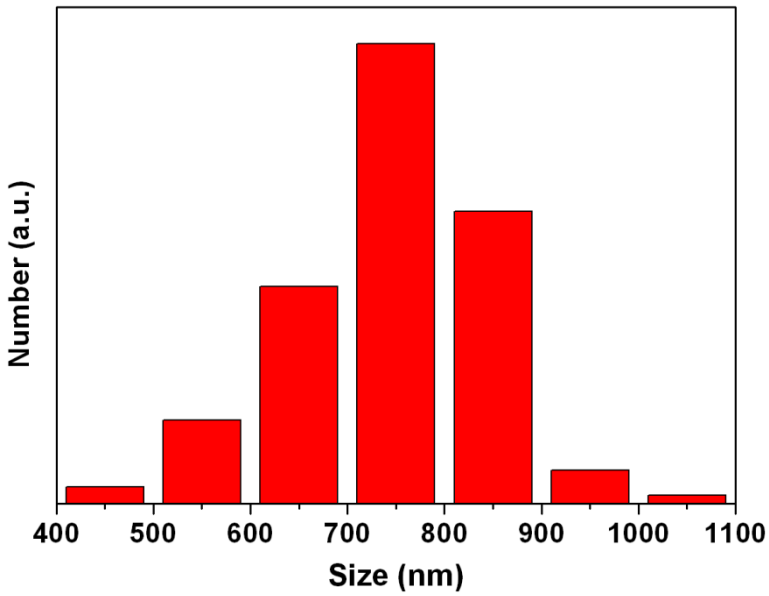

Fig. S4. Size distribution of 800 nm ZIF-67 (from a total number of 400).

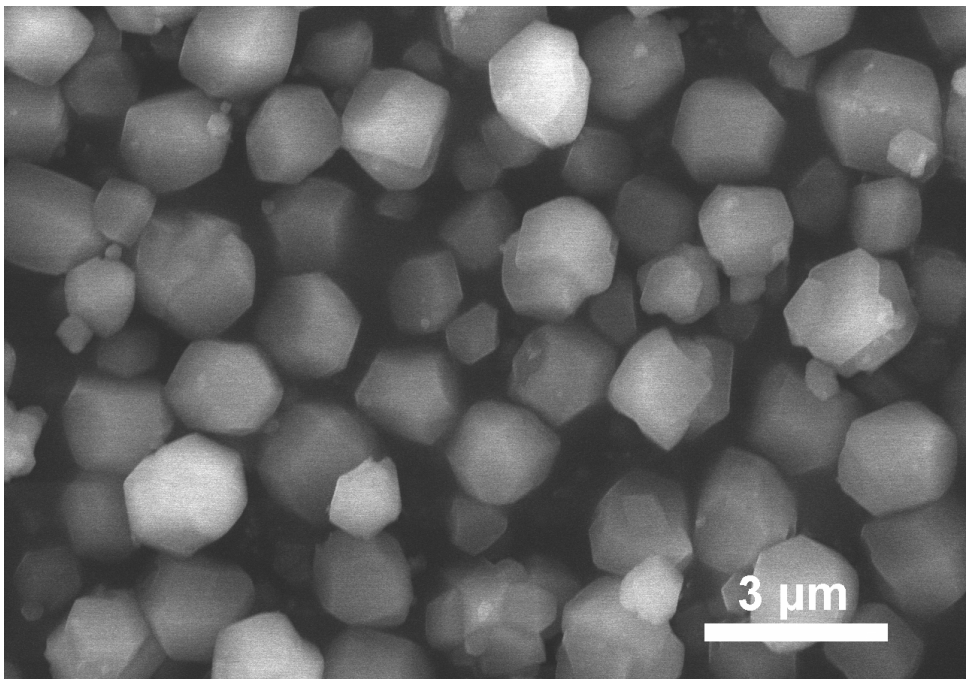

Fig. S5. SEM images of 1.7 μm ZIF-67.

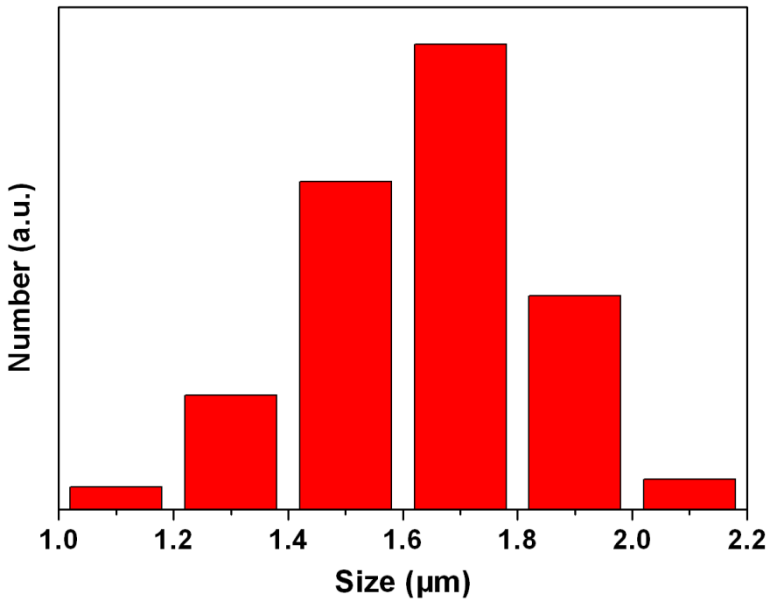

Fig. S6. Size distribution of 1.7 μm ZIF-67 (from a total number of 400).

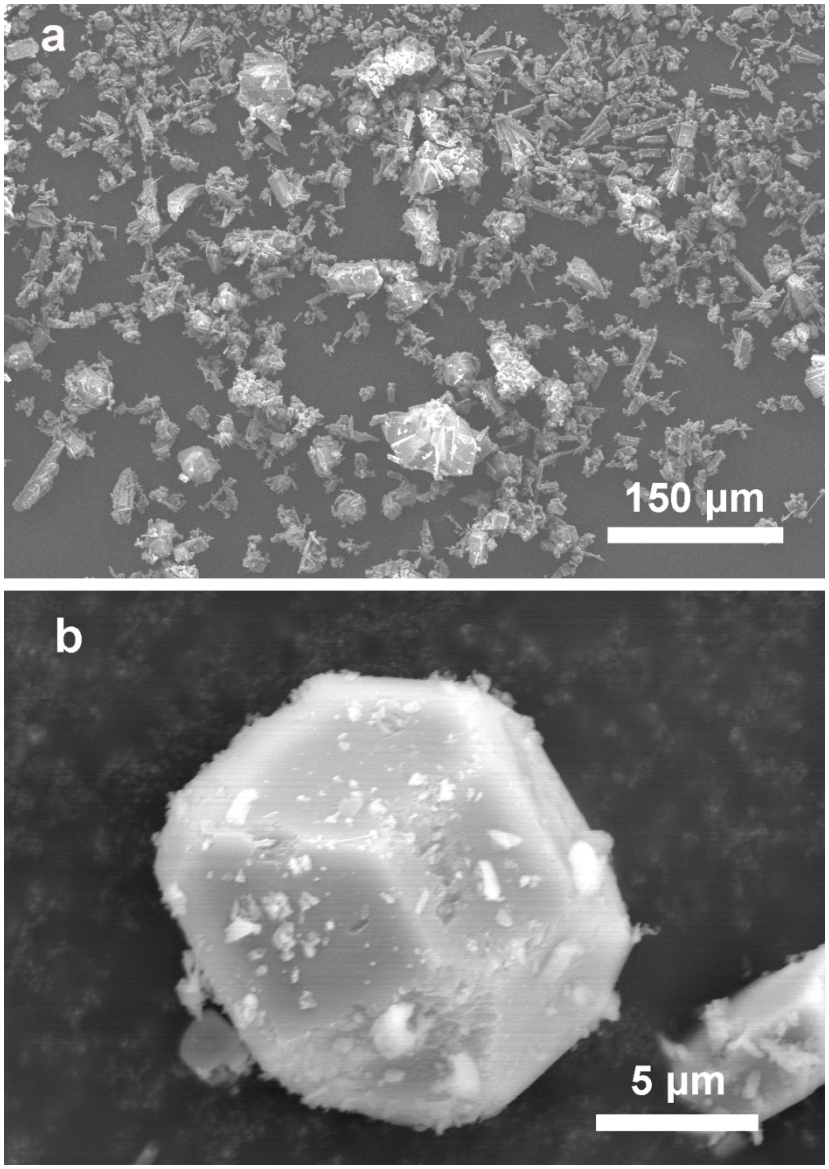

Fig. S7. SEM images of ZIF-67 bulk crystal prepared from solvothermal reaction.

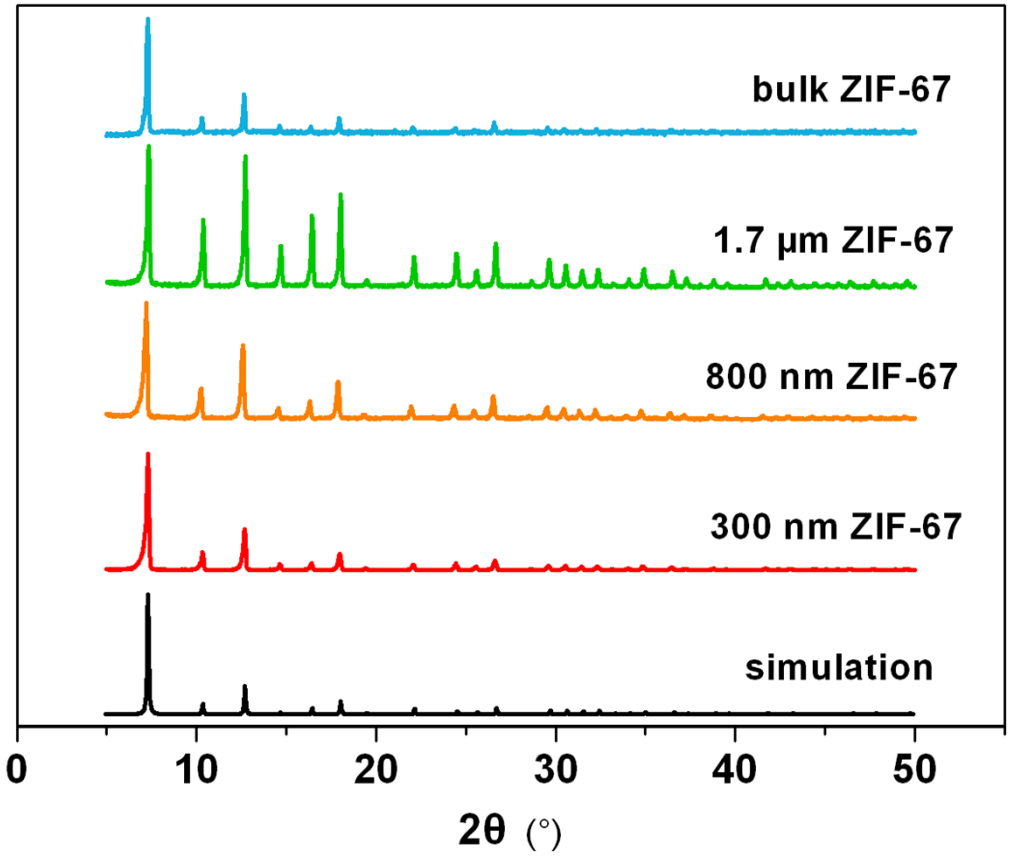

Fig. S8. XRD patterns of the as-prepared samples.

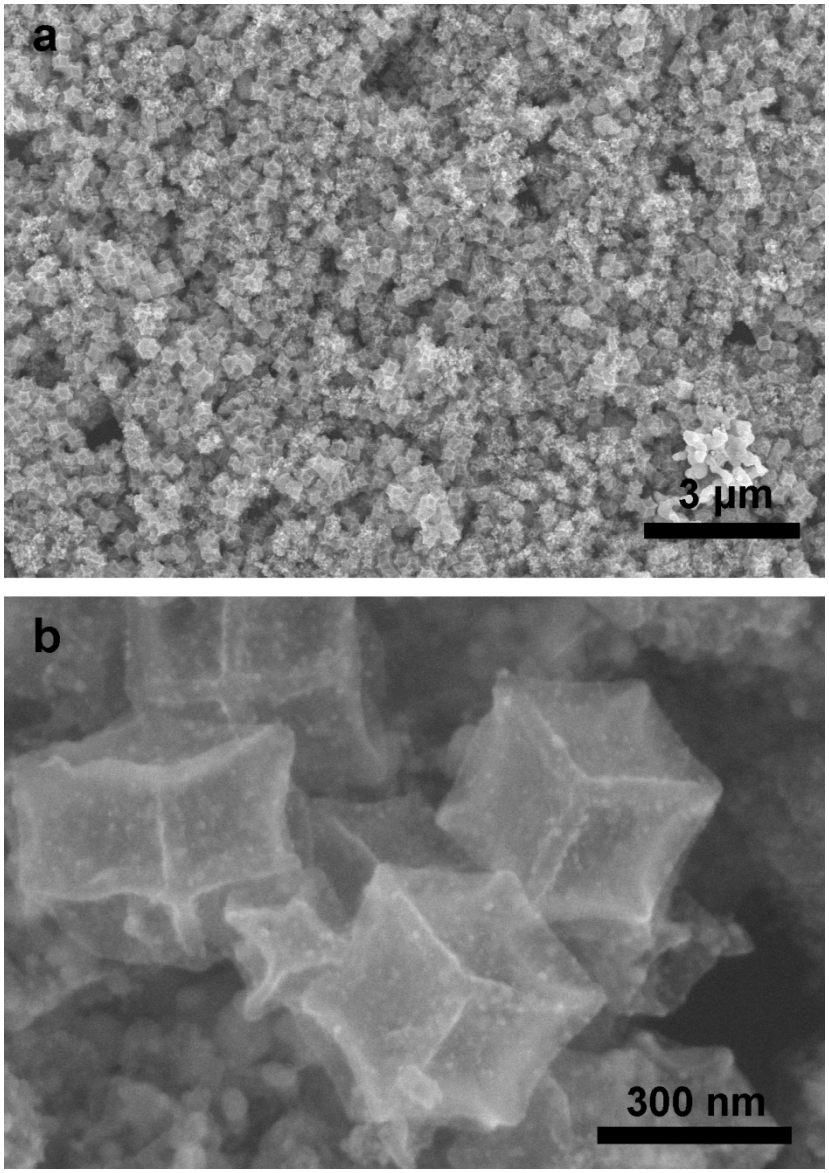

Fig. S9. SEM images of 300 nm ZIF-67 treated at 750 °C.

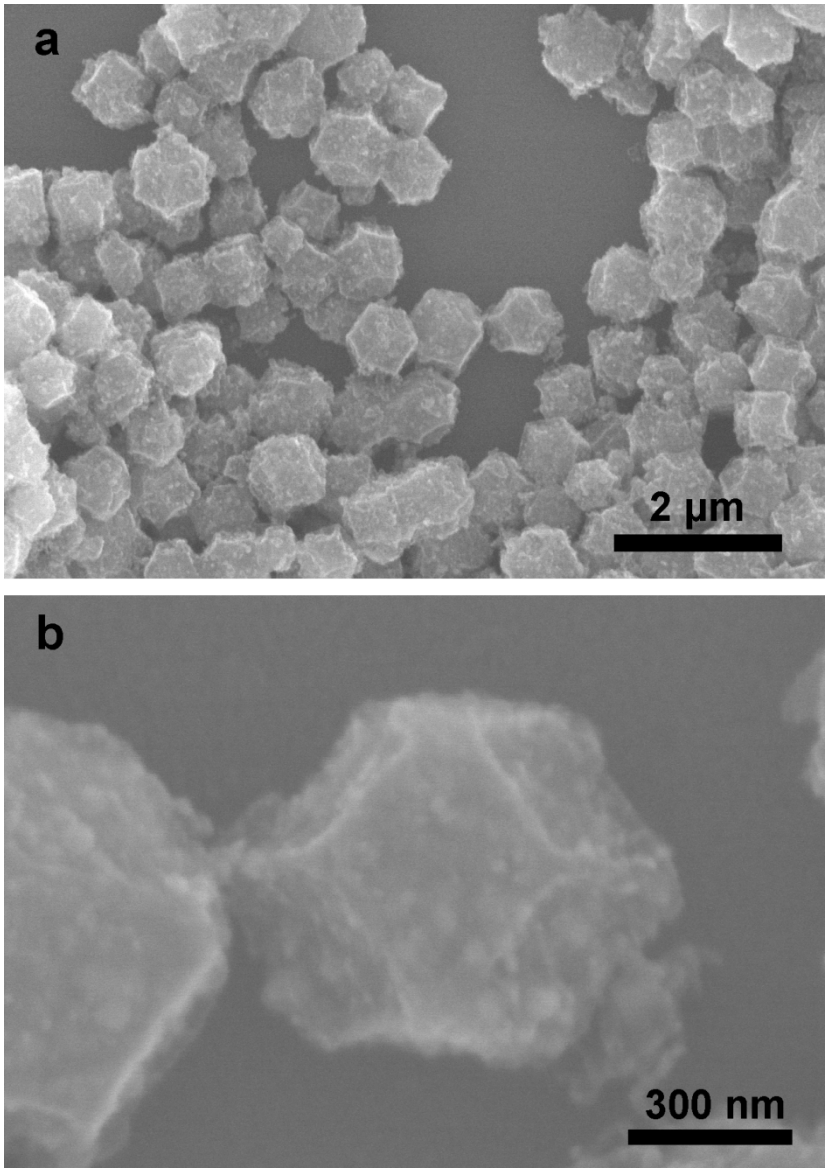

Fig. S10. SEM images of 800 nm ZIF-67 treated at 750 °C.

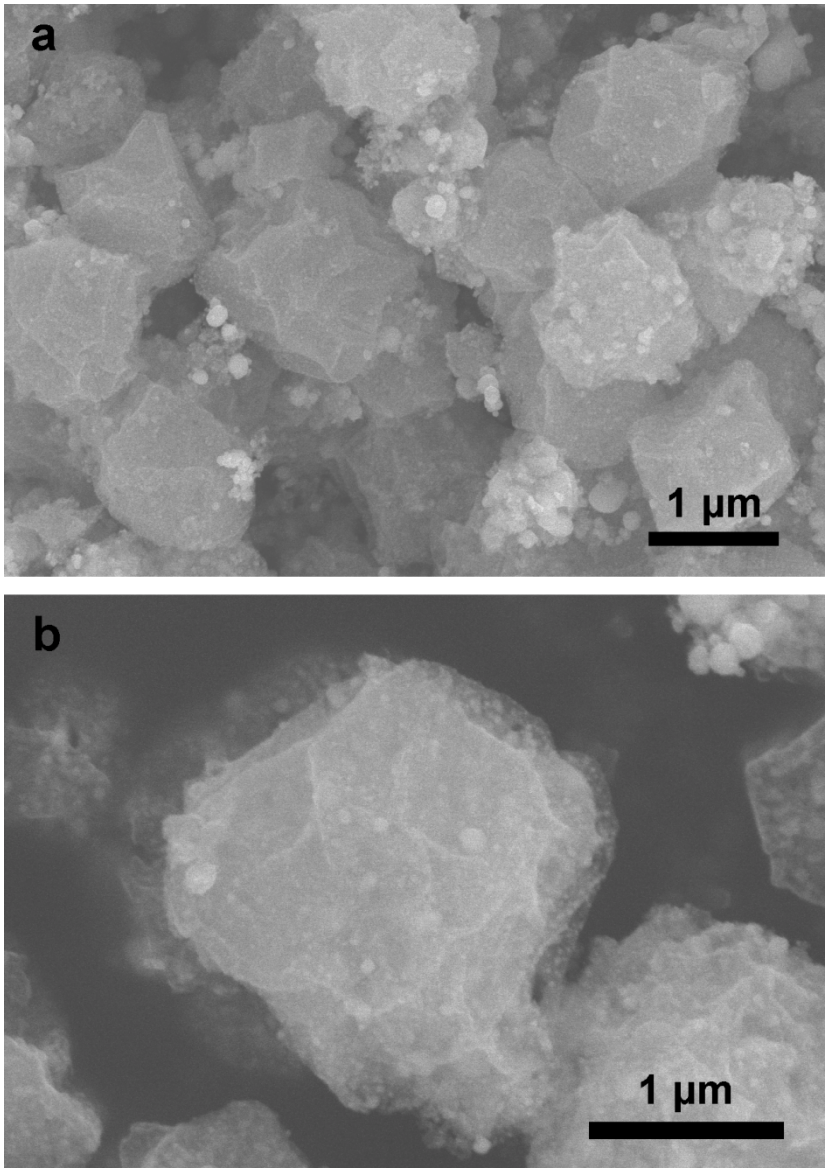

Fig. S11. SEM images of 1.7 μm ZIF-67 treated at 750 °C.

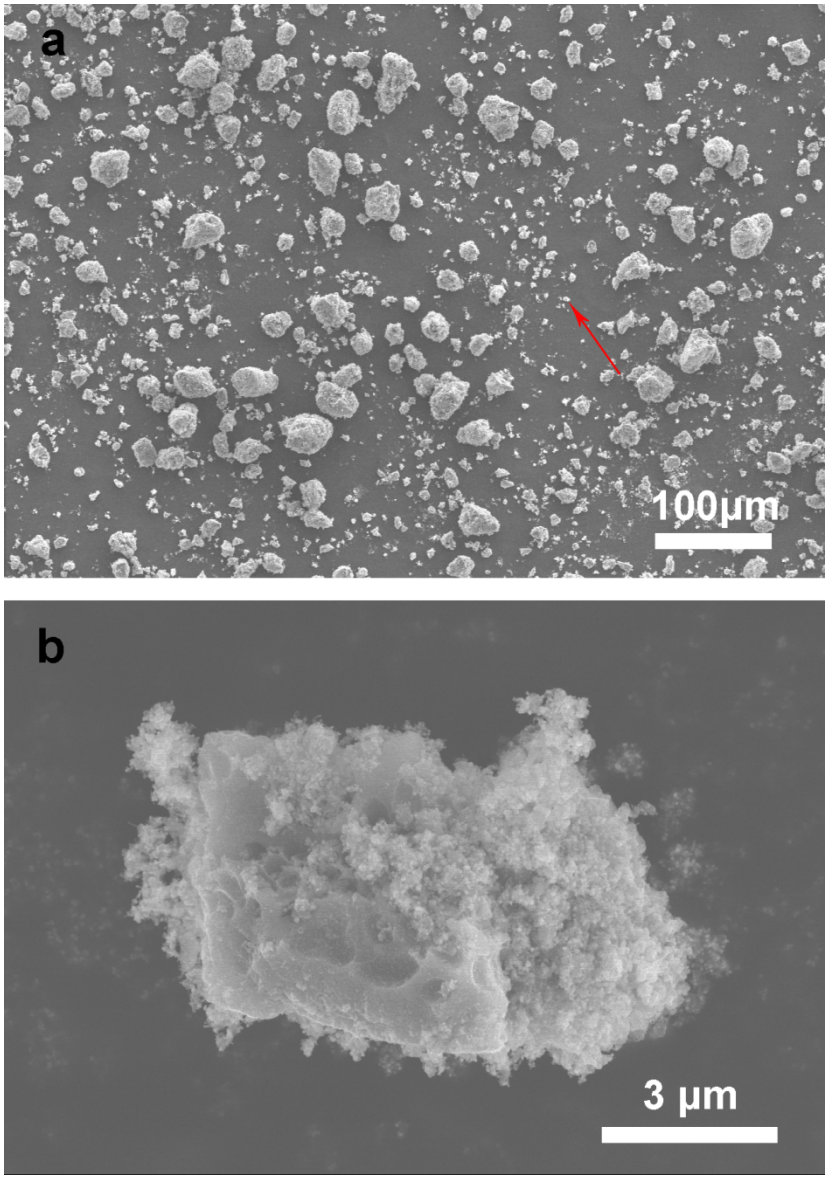

Fig. S12. SEM images of bulk ZIF-67 treated at 750 °C. The small particle (red arrow in a) is displayed at a higher magnification in b.

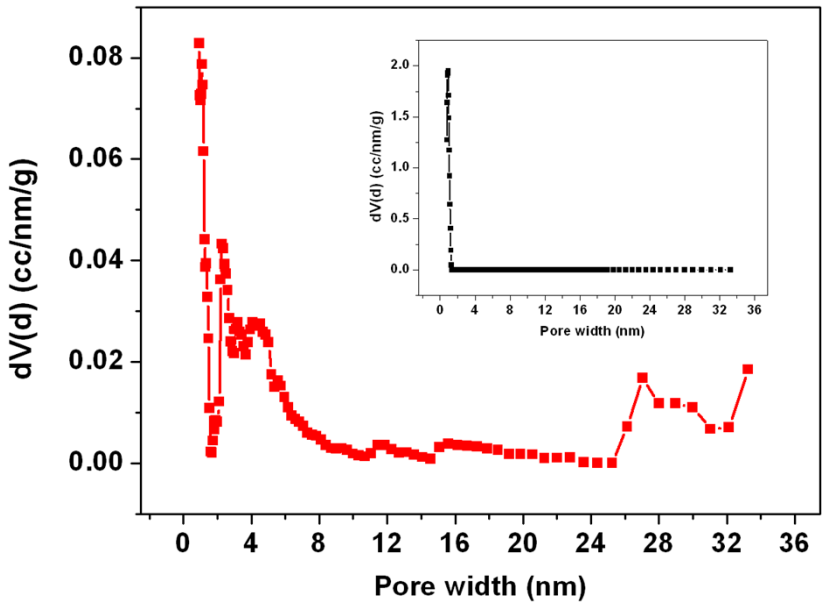

Fig. S13. Pore size distributions of 300 nm ZIF-67 before(inset) and after heat treatment at 750 °C.

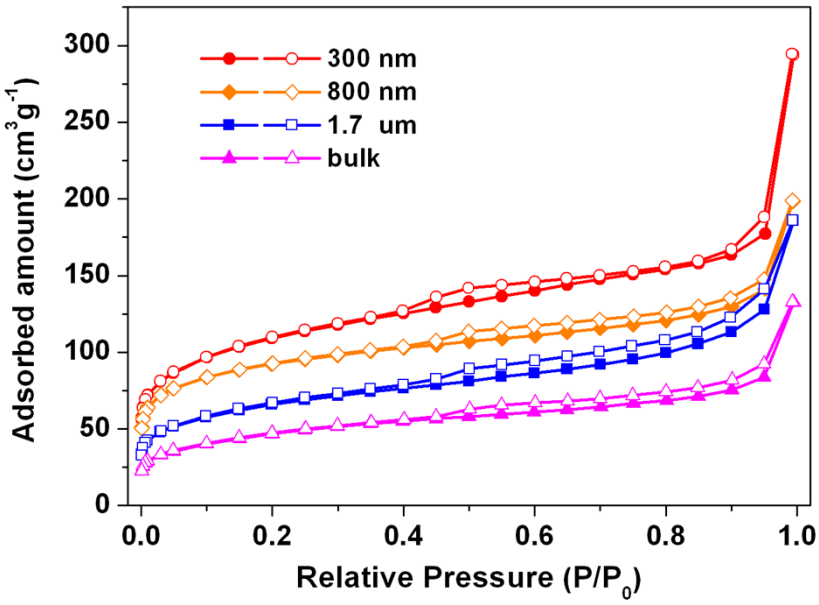

Fig. S14. Nitrogen sorption isotherms for MDC samples of different sizes. The solid and open symbols represent the adsorption and desorption branches, respectively. The BET surface areas of 300 nm, 800 nm, 1.7 μm and bulk MDCs are 386, 326, 233 and 165 m^2 g^{-1}, respectively.

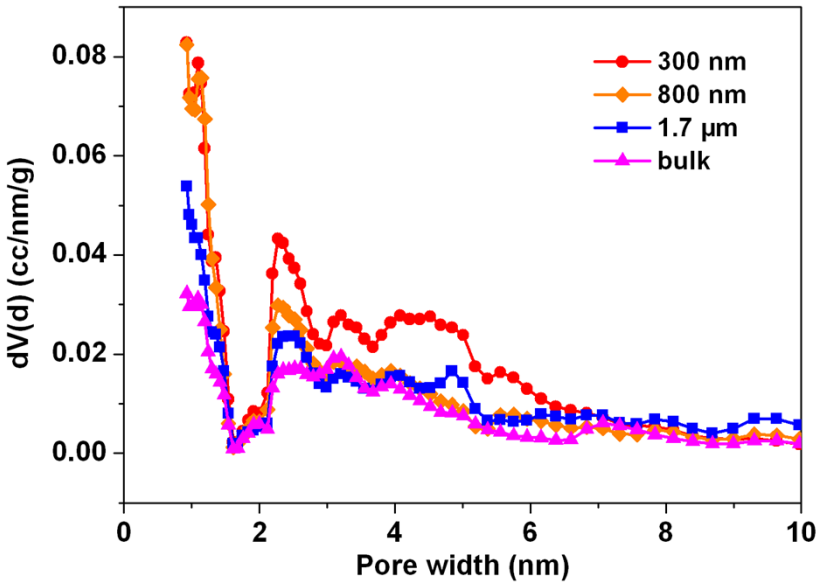

Fig. S15. Pore size distributions for MDC samples.

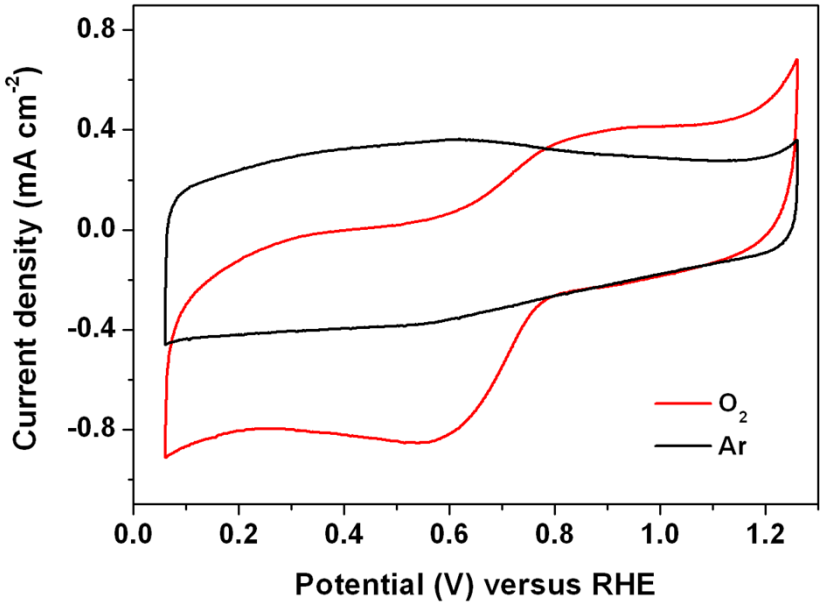

Fig. S16. CV of bulk ZIF-67 treated at 750 °C.

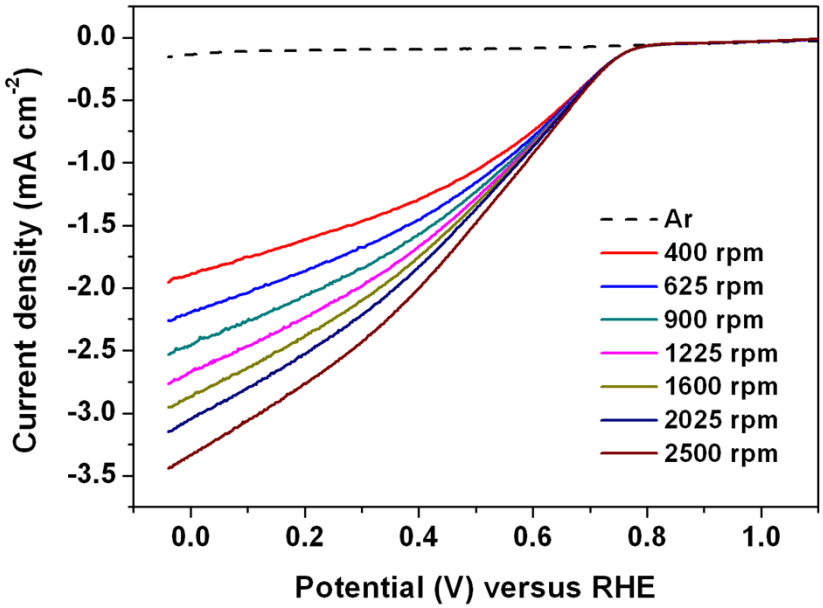

Fig. S17. RDE polarization curves of bulk ZIF-67 treated at 750 °C.

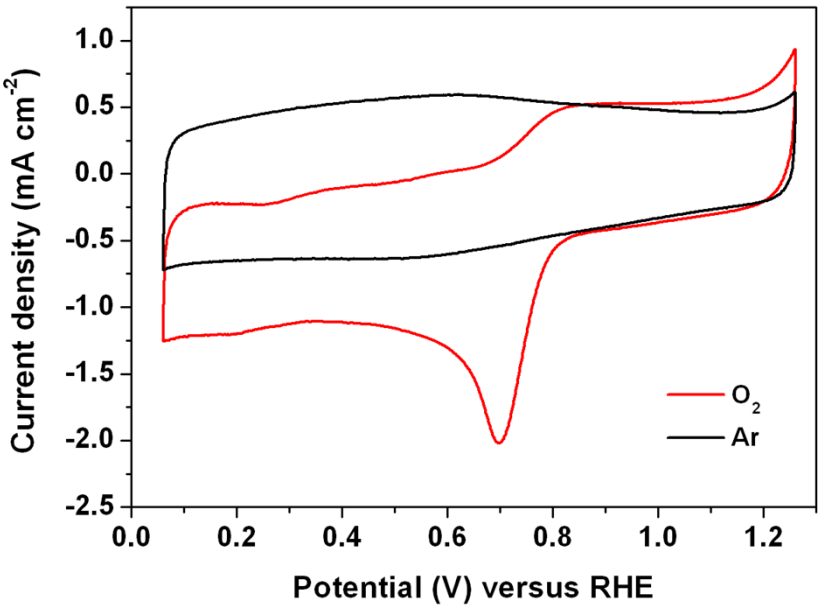

Fig. S18. CV of 1.7 μm ZIF-67 treated at 750 °C.

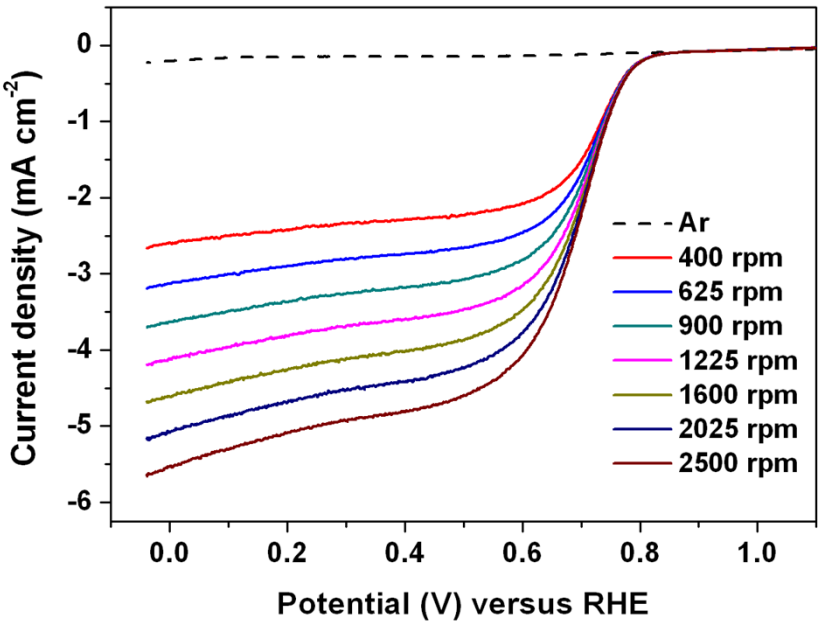

Fig. S19. RDE polarization curves of 1.7 μm ZIF-67 treated at 750 °C.

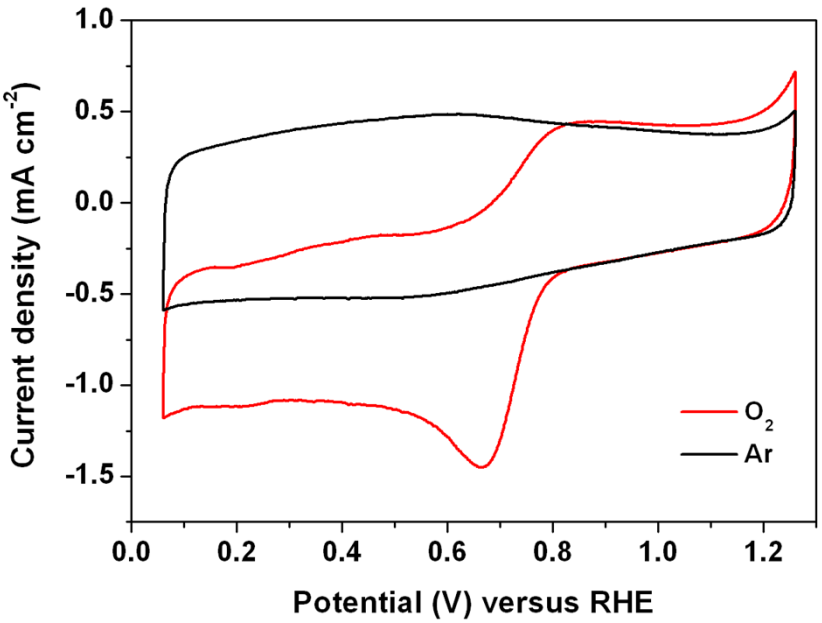

Fig. S20. CV of 800 nm ZIF-67 treated at 750 °C.

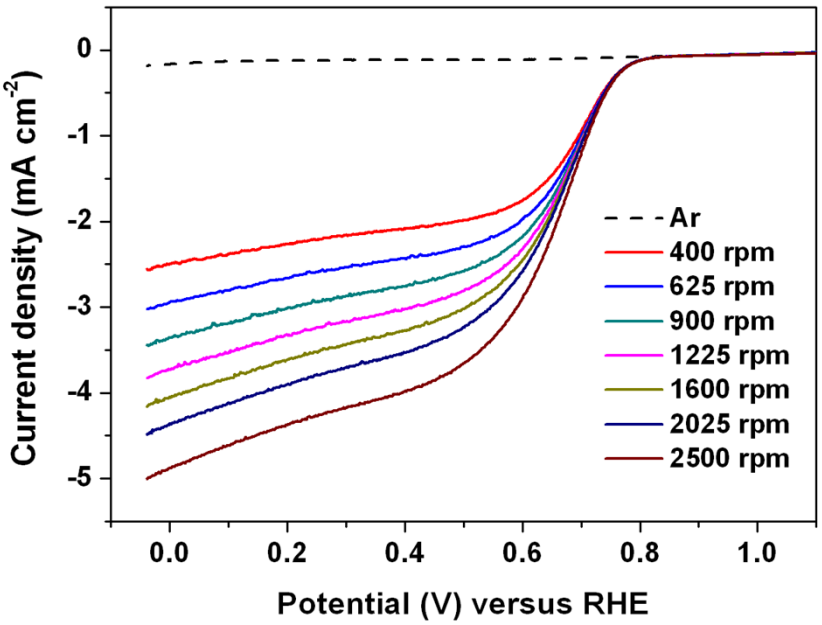

Fig. S21. RDE polarization curves of 800 nm ZIF-67 treated at 750 °C.

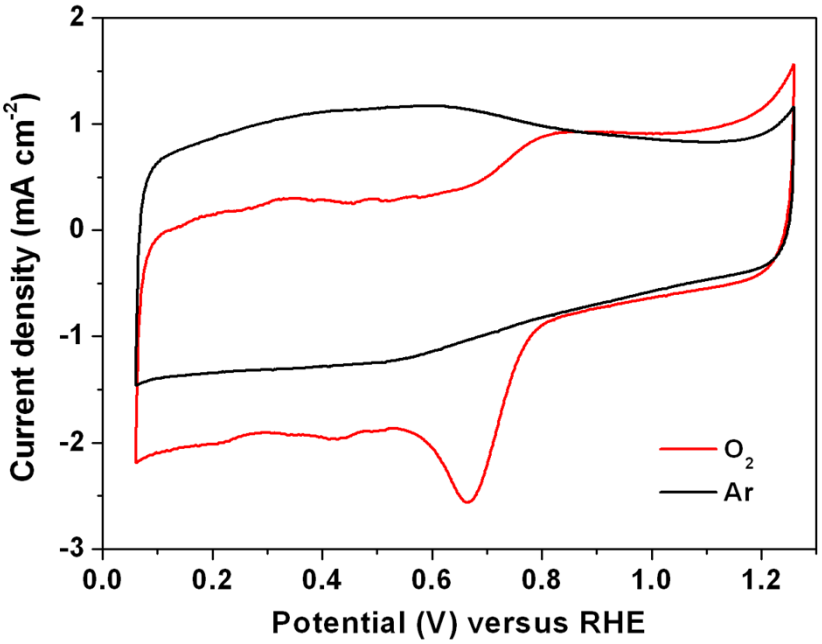

Fig. S22. CV of 300 nm ZIF-67 treated at 750 °C.

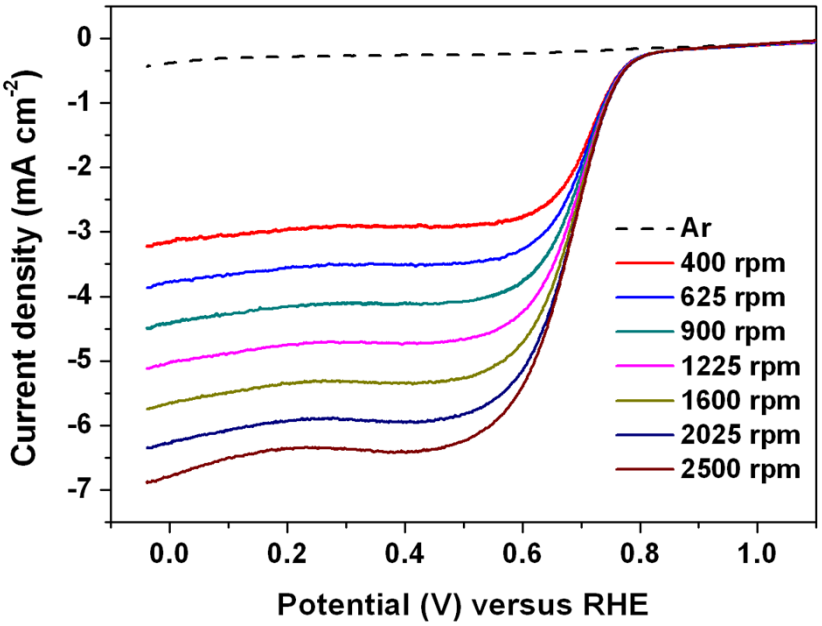

Fig. S23. RDE polarization curves of 300 nm ZIF-67 treated at 750 °C.

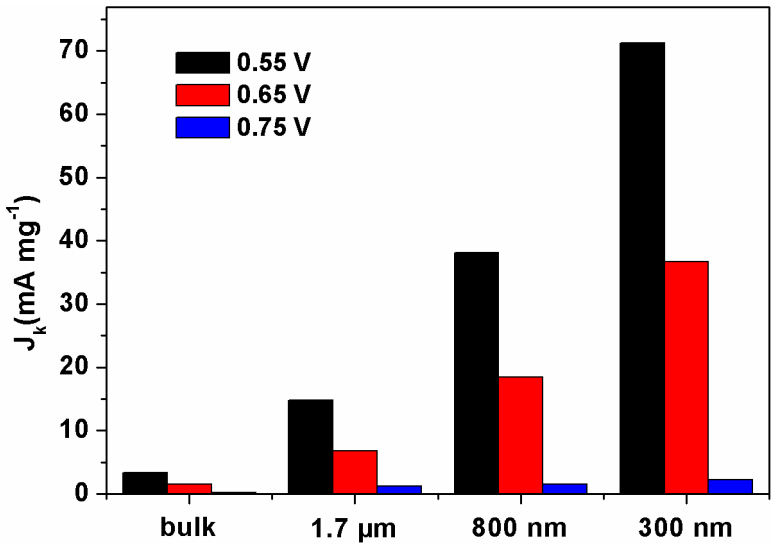

Fig. S24. Mass activities at various potentials for MDCs of different sizes.

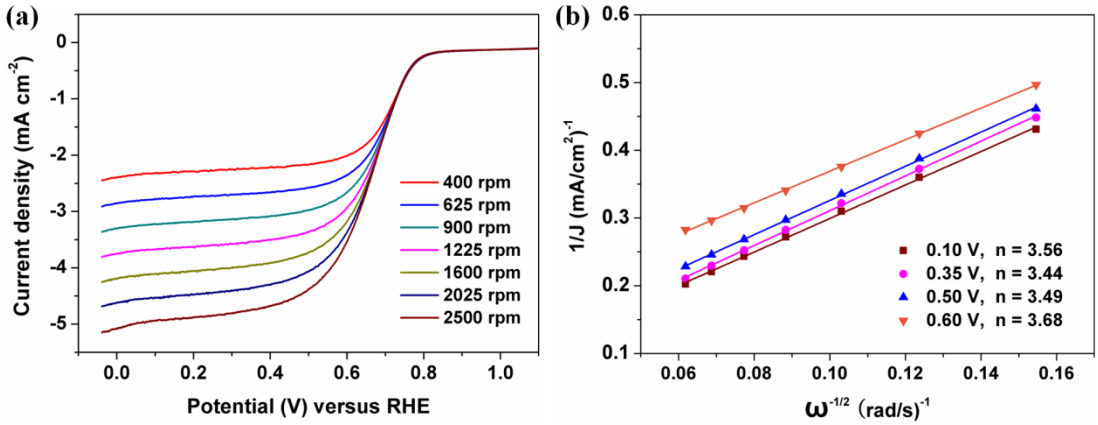

Figure S25. (a) RDE polarization curves of 300 nm ZIF-67 treated at 750 °C at catalyst loading of 0.1 mg cm^{-2}. (d) Corresponding Koutecky-Levich plots at different potentials.

Heat treatment temperature effect on ORR activity

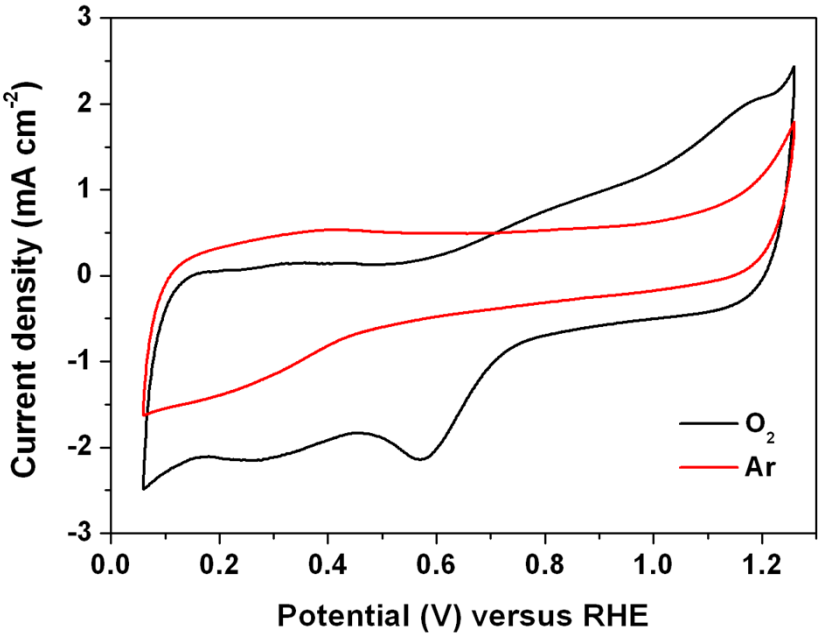

Fig. S26. CV of 300 nm ZIF-67 treated at 600 °C.

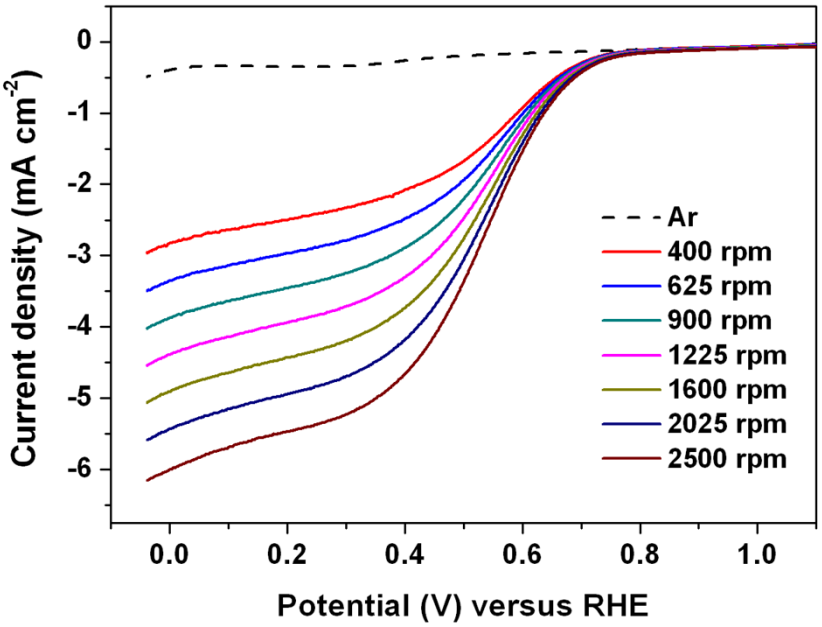

Fig. S27. RDE polarization curves of 300 nm ZIF-67 treated at 600 °C.

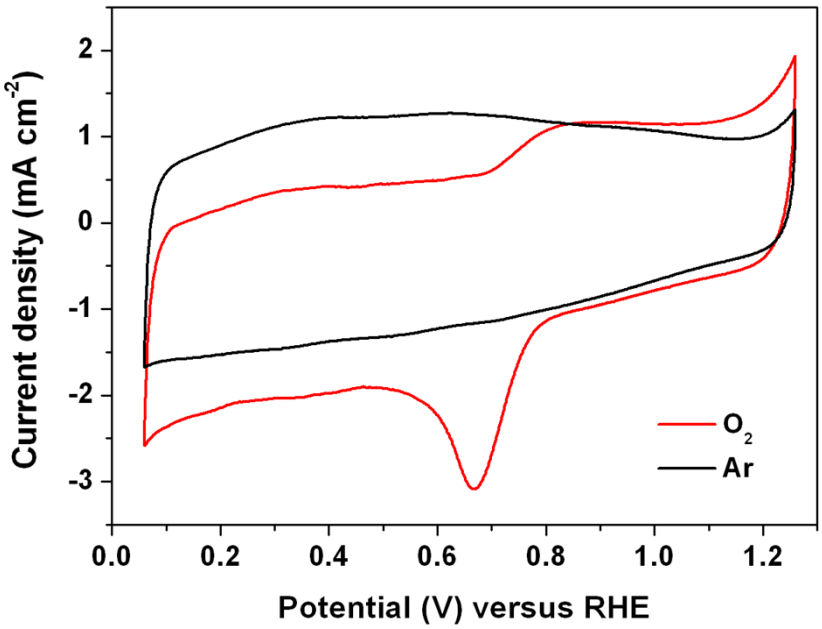

Fig. S28. CV of 300 nm ZIF-67 treated at 700 °C.

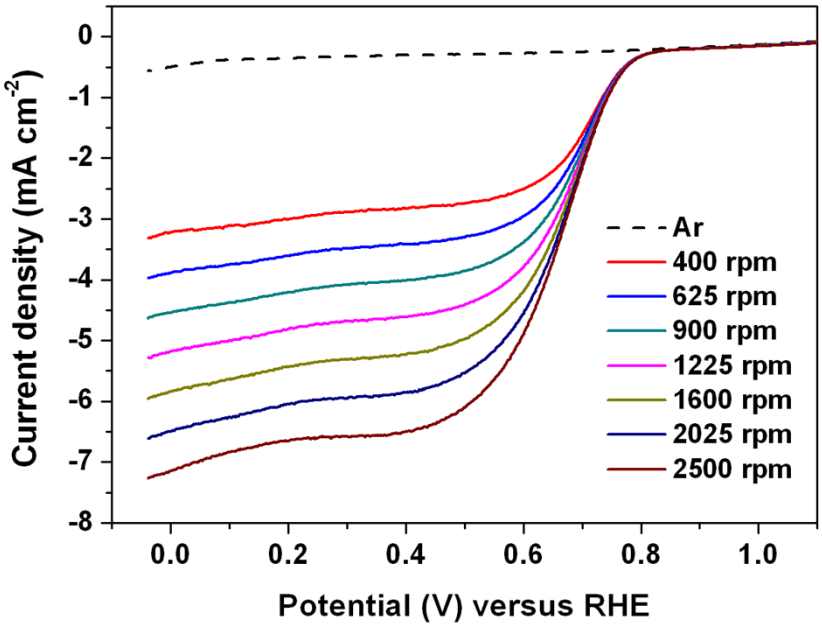

Fig. S29. RDE polarization curves of 300 nm ZIF-67 treated at 700 °C.

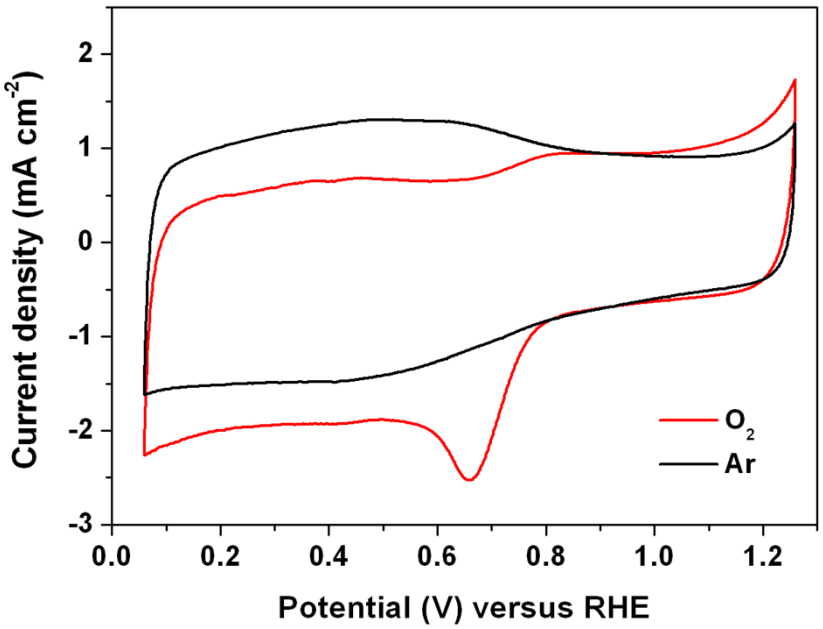

Fig. S30. CV of 300 nm ZIF-67 treated at 800 °C.

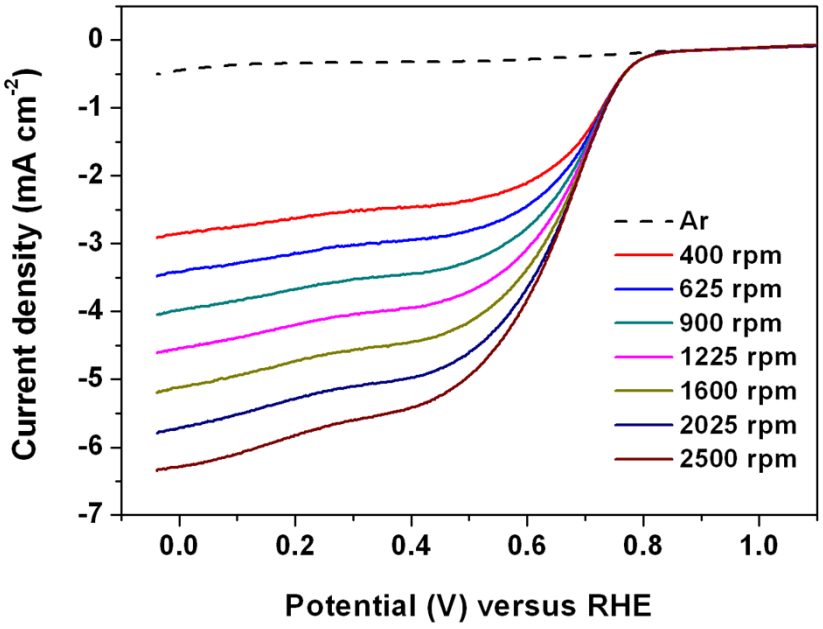

Fig. S31. RDE polarization curves of 300 nm ZIF-67 treated at 800 °C.

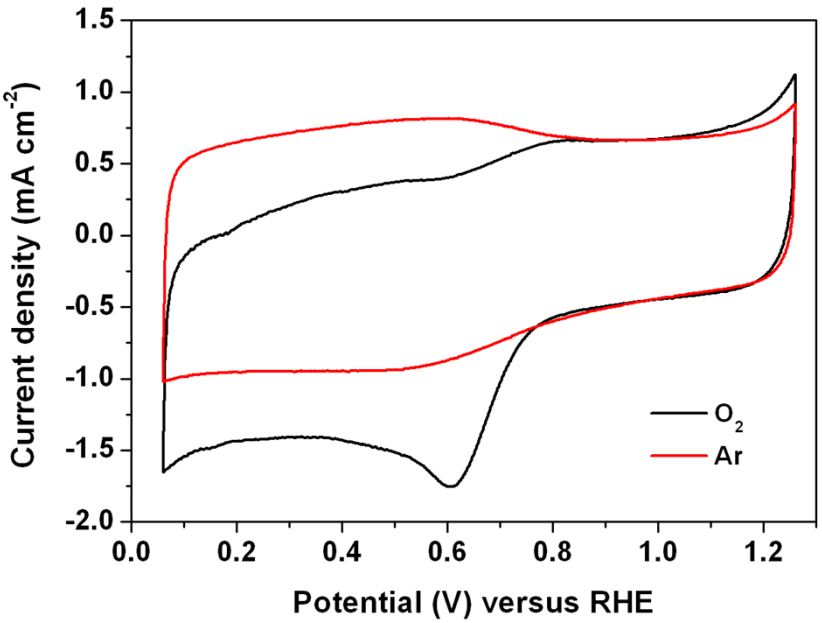

Fig. S32. CV of 300 nm ZIF-67 treated at 900 °C.

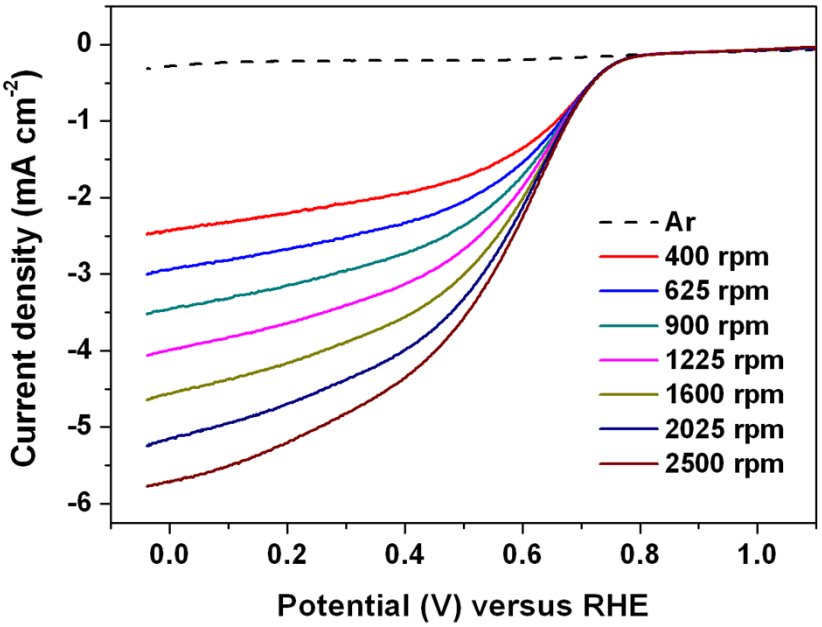

Fig. S33. RDE polarization curves of 300 nm ZIF-67 treated at 900 °C.

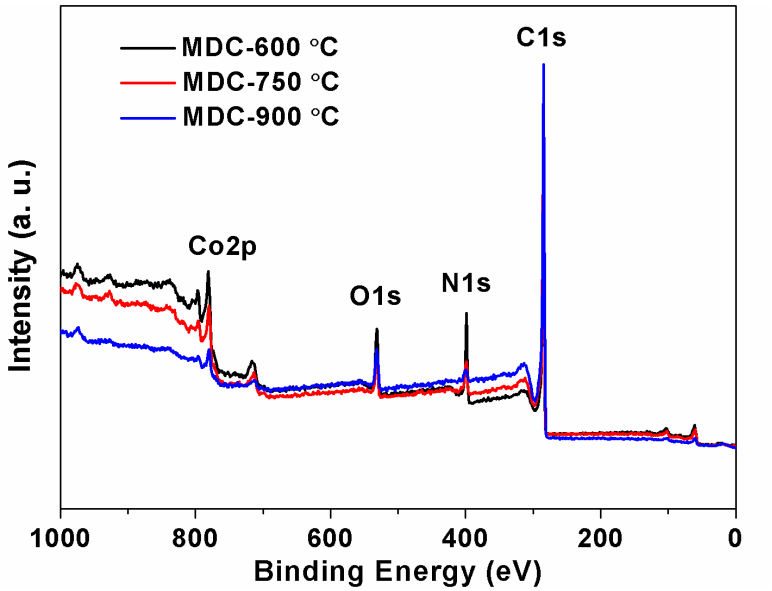

Fig. S34. XPS full spectra of MOF derived catalysts prepared at different temperatures.

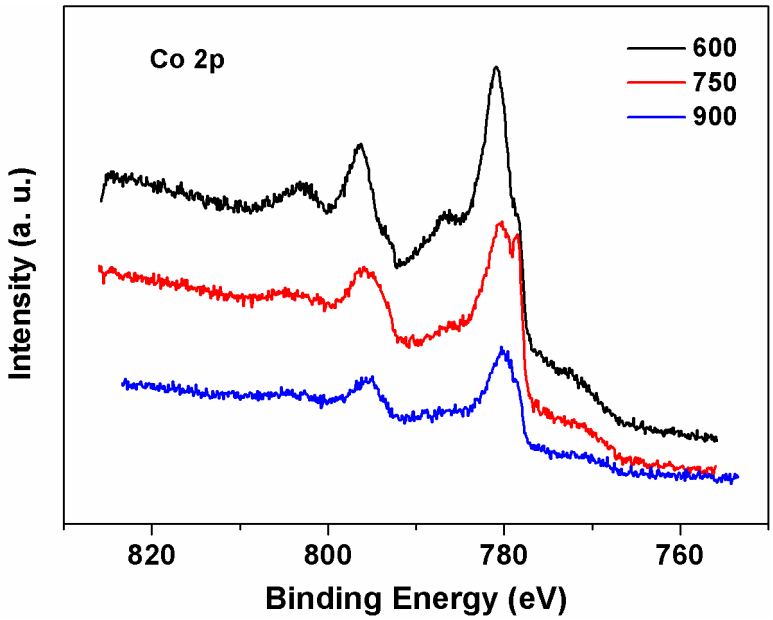

Fig. S35. Co 2p XPS spectra of MDC prepared at 600 °C, 750 °C and 900 °C.

Table S1. Performances of the reported ORR catalysts in acidic media.

Sample	Electrolyte	Onset potential	Half-wave potential	Ref.
MDC	0.1 M $HClO_4$	0.86 V	0.71 V	This work
N-CX	0.5 M H_2SO_4	0.81 V	0.65 V [a]	2
$Co_{0.5}Mo_{0.5}O_yN_z/C$	0.1 M $HClO_4$	0.645 V	0.413 V	3
CoP-CMP800	0.5 M H_2SO_4	0.74 V	0.64 V	4
C-N-Co	0.5 M H_2SO_4	0.87 V [a]	0.79 V	5
C-N-Fe	0.5 M H_2SO_4	0.84 V	0.73 V	5
1-750	0.1 M $HClO_4$	0.83 V	0.68 V	6
$Co_{1-x}S$/RGO	0.5 M H_2SO_4	0.80 V	0.60 V [a]	7

[a] This value is not given but read from the RDE curve.

Table S2. Element content of MOF derived catalysts prepared at different temperatures.[a]

catalyst	C (at %)	Co (at %)	N (at %)	O (at %)
MDC-600 °C	74.77	3.96	13.87	7.41
MDC-750 °C	86.31	2.56	6.40	4.73
MDC-900 °C	90.69	1.19	2.91	5.21

[a] The element content is measured using XPS.

Reference:

1 Y. Y. Liang, Y. G. Li, H. L. Wang, J. G. Zhou, J. Wang, T. Regier and H. J. Dai,

Nat. Mater., 2011, **10**, 780.

2 H. Jin, H. M. Zhang, H. X. Zhong and J. L. Zhang, *Energy Environ. Sci.*, 2011, **4**, 3389.

3 B. F. Cao, G. M. Veith, R. E. Diaz, J. Liu, E. A. Stach, R. R. Adzic and P. G. Khalifah, *Angew. Chem. Int. Ed.,* 2013, **52**, 10753.

4 Z. S. Wu, L. Chen, J. Z. Liu, K. Parvez, H. W. Liang, J. Shu, H. Sachdev, R. Graf, X. L. Feng and K. Müllen, *Adv. Mater.,* 2014, **26**, 1450.

5 H. W. Liang, W. Wei, Z. S. Wu, X. L. Feng and K. Müllen, *J. Am. Chem. Soc.*, 2013, **135**, 16002.

6 S. Q. Ma, G. A. Goenaga, A. V. Call and D. J. Liu, *Chem. Eur. J.,* 2011, **17**, 2063.

7 H. L. Wang, Y. Y. Liang, Y. G. Li and H. J. Dai, *Angew. Chem. Int. Ed.*, 2011, **50**, 10969.